URSI GASS 2021, Rome, Italy, 28 August - 4 September 2021

The Impact of Self-resonance on Self-inductance and Mutual Inductance of Two Coils used for Wireless Power Transfer

Yuxin Zhang* (1), Huapeng Zhao(1), Jun Hu(1), Jiafeng Zhou(2), and Zhizhang (David) Chen(3)
(1) University of Electronic Science and Technology of China, Chengdu, China
(2) University of Liverpool, Liverpool, United Kingdom
(3) Fuzhou University, Fujian, China on leave from Dalhousie University, Halifax, Canada

Abstract

Due to distributed capacitance, a planar printed coil has self-resonance, which will significantly affect self-inductance and mutual inductance. In this paper, the impact of self-resonance on self-inductance and mutual inductance of two coils is analyzed by the equivalent circuit, and the calculations of apparent self-inductance and apparent mutual inductance are derived. The analysis results can well explain the frequency characteristics of the planar printed coils' self-inductance and mutual inductance obtained by full-wave simulation. Finally, the correctness of the analysis results derived from the equivalent circuit has been verified by the numerical example.

1 Introduction

Wireless power transfer (WPT) is used in portable electronic devices [1], implantable medical devices [2], electric vehicles [3], and so on. It is subject to intensive research by both academia and industry. The planar printed coil is a preferred WPT coil due to its low-profile, low-cost, and convenience for producing and assembling.

Due to its distributed capacitance, the planar printed coil has self-resonance [4-5]. In terms of sizes, high-frequency WPT is preferred. However, the higher frequency, the more significant the effect of the self-resonance becomes. The self-resonance will affect not only the self-inductance but also the mutual inductance between two coils. Mutual inductance is crucial for magnetically coupled resonance (MCR) WPT and the wireless power transfer efficiency [6]. Consequently, it is necessary to evaluate the impact of self-resonance on the performances of two WPT planar coils for WPT. The influence of self-resonance on the single planar printed coil has been studied [4-5], but not two coupling coils.

This paper's main contribution is to analyze the impact of self-resonance on self-inductance and mutual inductance of two planar printed coils. By using the full-wave simulations, the impact of self-resonance on self-inductance and mutual inductance of two coils is analyzed with the equivalent circuit. The analysis results derived from the equivalent circuit can well explain the frequency characteristics of self-inductance and mutual inductance.

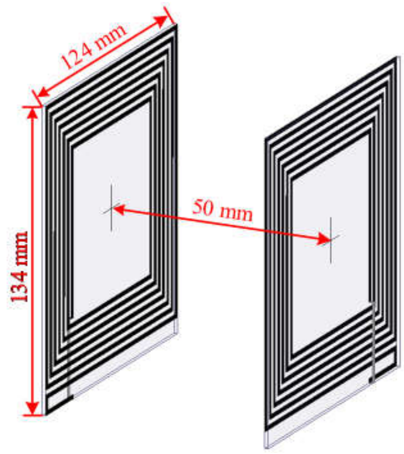

Figure 1. The illustration of two identical planar printed coils with the width of 2 mm, the gap of 2 mm, the FR4 dielectric, dielectric of 1.6 mm. The two coils are placed 50 mm apart.

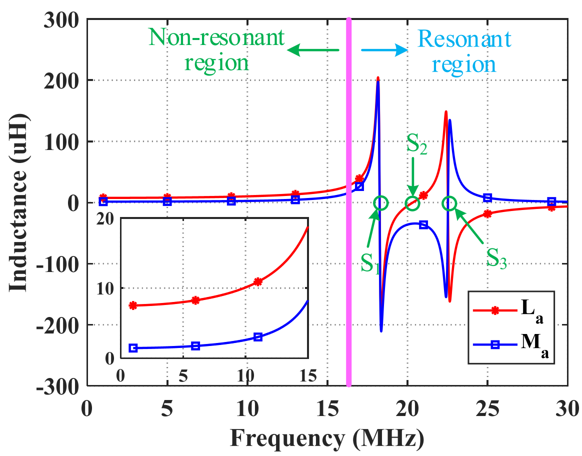

Figure 2. The apparent self-inductance L_a and apparent mutual inductance M_a of the two planar coils obtained with full-wave simulation.

2 Impact of Self-resonance on Two Coils

Fig. 1 presents the configuration of the two coils under study. The apparent self-inductance L_a and apparent mutual inductance M_a versus frequency were simulated with full-wave simulations, and the results are shown in

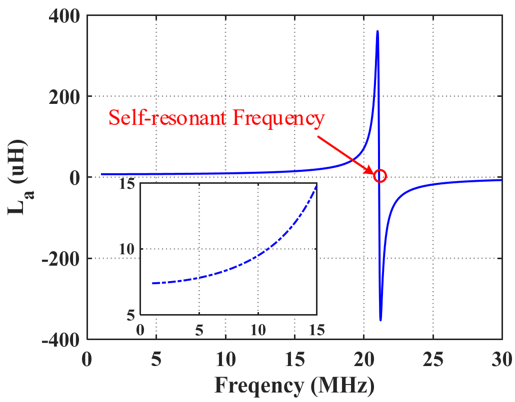

Figure 3. The apparent self-inductance L_a of the single planar printed coil versus frequency obtained with full-wave simulation.

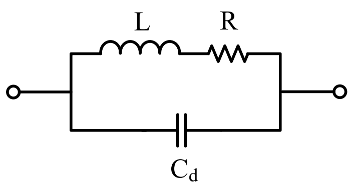

Figure 4. The equivalent circuit of the planar printed coil.

Fig. 2. The following formulas are used to compute L_a and M_a

$$L_a = \frac{\mathrm{Im}(Z_{11})}{\omega} \tag{1}$$

$$M_a = \frac{\mathrm{Im}(Z_{21})}{\omega} = \frac{\mathrm{Im}(Z_{12})}{\omega} \tag{2}$$

where 'Im' means taking the imaginary part, Z_{11} is the self-impedance, Z_{21} and Z_{12} are the mutual impedance, and ω is the angular frequency. From Fig. 2, it is seen that below 18 MHz, L_a and M_a have similar variations versus frequency. Beyond 18 MHz, L_a has three zero points (S_1, S_2, and S_3), and M_a has two zero points (S_1 and S_3). Both L_a and M_a have jumps in values at S_1 and S_3, which indicate a parallel RLC resonance, while L_a has a smooth change at S_2, which corresponds to a series RLC resonance. These resonances are due to the unremovable distributed capacitances of the coils. In the design of WPT system, the operating frequency should be avoided in the resonant region as far as possible.

For comparison purposes, the apparent self-inductance L_a of the single planar printed coil (with the same dimension as the coil shown in Fig. 1) was simulated with full-wave simulation. The results are shown in Fig. 3. From Fig. 3, it is seen that L_a slowly increases with frequency until the frequency reaches 21 MHz. At 21 MHz, L_a changes abruptly, which corresponds to a parallel RLC resonance. Again the resonance is due to the unremovable distributed capacitances of the coil.

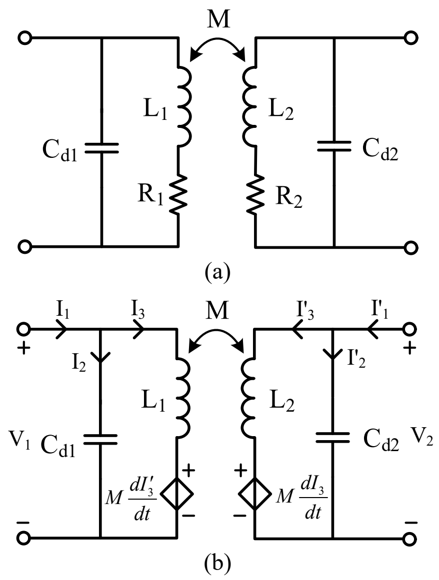

Figure 5. (a) The equivalent circuit of the two coupling coils. (b) The mutual inductance is decoupled by the equivalent voltage source.

As seen from the above figures, both the self-inductance and mutual inductances have self resonances, like that with the single planar printed coil [4-5]. As a result, while the circuit of Fig. 4 can represent the equivalent circuit of the single planar coil, the circuit of Fig. 5 can represent the equivalent circuit of the two coupling coils.

The single planar printed coil can be equivalent to an RLC parallel resonant circuit as shown in Fig. 4 [7], where L is the true self-inductance (different from L_a), R is the loss resistance, and C_d is called the distributed capacitance. The coupling between adjacent conductors results in the distributed capacitance [7]. Assuming that the coil is lossless, L_a of the equivalent circuit shown in Fig. 4 can be written as follows

$$L_a = \frac{\mathrm{Im}(Z_{11})}{\omega} = \frac{L}{1-\omega^2 C_d L} \tag{3}$$

It is evident that the apparent self-inductance L_a is a function of the distributed capacitance and the operating frequency and differs from the true or low-frequency self-inductance L. There is a singular point in L_a, when ω equals to $\left[\sqrt{C_d L}\right]^{-1}$. This singular point is the self-resonant frequency shown in Fig. 3, which will significantly affect L_a. As the frequency goes closer to the self-resonant frequency, the change of L_a becomes more and more drastic.

In the next section, the impact of self-resonance on the two coupling coils is analyzed based on the single coil's parallel resonant equivalent circuit.

3 Analysis Based on Equivalent Circuit

The influence of self-resonance on two coupling coils is analyzed by using the equivalent circuit mentioned in Fig. 3. The equivalent circuit of two coupling coils is shown in Fig. 5 (a), where M is mutual inductance between two coils. Note that no tuning capacitor is added in this system, and the parallel capacitors C_{d1} and C_{d2} are the distributed capacitance caused by the coils' structures. It should be pointed out that M_a obtained with the full-wave simulation is different from the true mutual inductance M; M_a contains three parts: coils' true mutual inductance M, self-resonance, and capacitive coupling between two coils. Since the capacitive coupling between two coils is small, the equivalent circuit model, as shown in Fig. 5 (a), ignores the capacitive coupling between two coils.

The mutual inductance M in Fig. 5 (a) is decoupled with the equivalent voltage source, as shown in Fig. 5 (b). In order to simplify the calculation and derivation, two coils are assumed lossless (R_1=R_2=0), because the loss resistance of the coil is usually less than 5 Ω. To facilitate the subsequent analysis, the port voltage and branch current are denoted as shown in Fig. 5 (b).

Based on Kirchhoff's law of voltage and current, six equations are obtained as follows:

$$V_1 = I_2 \bullet \frac{1}{j\omega C_{d1}} \tag{4}$$

$$V_1 = I_3 \bullet j\omega L_1 + I_3' \bullet j\omega M \tag{5}$$

$$I_1 = I_2 + I_3 \tag{6}$$

$$V_2 = I_2' \bullet \frac{1}{j\omega C_{d2}} \tag{7}$$

$$V_2 = I_3' \bullet j\omega L_2 + I_3 \bullet j\omega M \tag{8}$$

$$I_1' = I_2' + I_3' \tag{9}$$

By combining these six equations, the impedance matrix Z of the dual-port network can be written as follows:

$$\begin{bmatrix} V_1 \\ V_2 \end{bmatrix} = \begin{bmatrix} Z_{11} & Z_{12} \\ Z_{21} & Z_{22} \end{bmatrix} \begin{bmatrix} I_1 \\ I_1' \end{bmatrix} \tag{10}$$

$$Z_{11} = j\frac{\omega\left[L_1\left(1-\omega^2 C_{d2}L_2\right)+\omega^2 M^2 C_{d2}\right]}{\left(1-\omega^2 C_{d1}L_1\right)\left(1-\omega^2 C_{d2}L_2\right)-\omega^4 M^2 C_{d1}C_{d2}} \tag{11}$$

$$Z_{22} = j\frac{\omega\left[L_2\left(1-\omega^2 C_{d1}L_1\right)+\omega^2 M^2 C_{d1}\right]}{\left(1-\omega^2 C_{d1}L_1\right)\left(1-\omega^2 C_{d2}L_2\right)-\omega^4 M^2 C_{d1}C_{d2}} \tag{12}$$

$$Z_{12} = Z_{21} = j\frac{\omega^2 M^2}{\left(1-\omega^2 C_{d1}L_1\right)\left(1-\omega^2 C_{d2}L_2\right)-\omega^4 M^2 C_{d1}C_{d2}} \tag{13}$$

Because the identical coils are selected (see Fig. 2), L_a calculated through Z_{11} or Z_{22} is the same. They can be computed with:

$$L_a = \frac{\left[L_1\left(1-\omega^2 C_{d2}L_2\right)+\omega^2 M^2 C_{d2}\right]}{\left(1-\omega^2 C_{d1}L_1\right)\left(1-\omega^2 C_{d2}L_2\right)-\omega^4 M^2 C_{d1}C_{d2}} \tag{14}$$

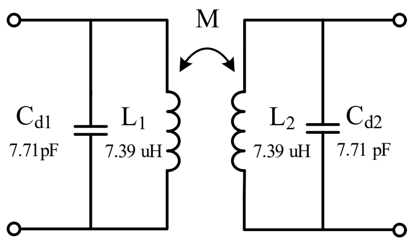

Figure 6. The equivalent circuit modeled from the two coupling coils shown in Fig. 1.

TABLE I

M AT DIFFERENT SEPARATIONS CALCULATED BY [8]

h (mm)	10	30	50	70
M (uH)	6.38	2.84	1.58	0.95

$$M_a = \frac{\omega M^2}{\left(1-\omega^2 C_{d1}L_1\right)\left(1-\omega^2 C_{d2}L_2\right)-\omega^4 M^2 C_{d1}C_{d2}} \tag{15}$$

The denominators of L_a and M_a are the same. Namely, both have the same resonant point. Set the denominators of (14) and (15) equal to zero, and the following equation can be obtained for the resonant frequencies:

$$\omega^4\left(C_{d1}C_{d2}L_1L_2 - M^2 C_{d1}C_{d2}\right) - \omega^2\left(C_{d1}L_1 + C_{d2}L_2\right) + 1 = 0 \tag{16}$$

Two positive roots and two negative roots can be obtained by solving (16). The two positive roots correspond to the singular point S_1 and S_3 of L_a and M_a in Fig. 2, which causes L_a and M_a sharp change at the frequency.

There are also zero points in L_a and no zero points in M_a (except ω=0); they are consistent with the simulation results in Fig. 2. Set the numerator of (14) equal to zero. The zero points of L_a can be found as

$$\omega\big|_{L_a=0} = \pm\sqrt{\frac{L_1}{C_{d2}L_1L_2 - M^2 C_{d2}}} \tag{17}$$

where the positive root corresponds to the zero point S_2 of L_a in Fig. 2. The parallel resonant equivalent circuit can well explain the singularity and zero point of L_a and M_a in full-wave simulation.

4 Simulation Verification

In order to verify the correctness of analysis results derived from the equivalent circuit, the planar printed coils' apparent mutual inductance M_a is modeled with the equivalent circuit. Accurate calculation of mutual inductance in the non-resonant region is more meaningful to guide the design of WPT system. Therefore, M_a in the non-resonant region is modeled in this section. The equivalent circuit parameters of the coil shown in Fig. 1 are obtained as follows.

Firstly, it is considered that the L_a obtained by full-wave simulation at low frequency (less than 1 MHz) is the ture self-inductance L of the coil. Therefore, L can be obtained

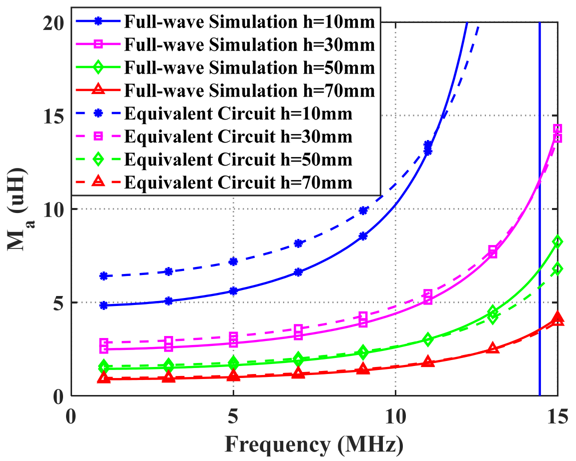

Figure 7. Comparison between the apparent mutual inductances M_a versus frequency computed by full-wave simulation and equivalent circuit.

from the simulation results of L_a in Fig. 3. Secondly, the distributed capacitance C_d can be calculated from the self-resonant frequency (21.1 MHz) in Figure 3 and (18).

$$\omega=\frac{1}{\sqrt{C_d L}} \tag{18}$$

The equivalent circuit of the two identical coils shown in Fig. 1 has been established, and the circuit parameters are shown in Fig. 6. The mutual inductance M in Fig. 6 is calculated by analytical formula [8] as shown in Table I. Note that central approximation is used to calculate M, assuming that all loops are located in the middle of the outermost and innermost loops. Different values of the separation h between the two coils are selected to further verify the effectiveness of the presented equivalent circuit.

Fig. 7 compared the apparent mutual inductances M_a computed by full-wave simulation and equivalent circuit. From Fig. 7, it can be observed that when the separation is large (h=70 mm), the M_a calculated by the full-wave simulation is in good agreement with that calculated by the equivalent circuit. When the separation is small (h=10 mm), the M_a calculated by full-wave simulation is different from that calculated by the equivalent circuit. This is because when the two coils are close to each other, the capacitive coupling between two coils is strong. The influence of capacitive coupling is considered in the full-wave simulation, while the presented equivalent circuit ignores it. To sum up, when the influence of capacitive coupling is small, the results calculated by presented equivalent circuit are in good agreement with the results of full-wave simulation, which proves the effectiveness of using the presented equivalent circuit to analyze the impact of self-resonance on mutual inductance.

5 Conclusion

This paper analyzed two planar printed coils' self-resonance by using the full-wave simulations and the equivalent circuit. The impact of the self-resonance on mutual inductance and self-inductance of two coils is analyzed. The single-coil self-resonance will result in the singularity of the two coils' impedance matrix, which will significantly affect mutual inductance and self-inductance of two coils. Therefore, the impact of self-resonance should be considered in a WPT system. Future work is to consider the capacitive coupling between two planar printed coils in the equivalent circuit and to extract the equivalent circuit of the planar printed coil accurately.

6 Acknowledgements

Sichuan Science and Technology Program supported this work under Grant No. 2021YFH0070 and the National Science Foundation of China under Grant No. 62071125.

7 References

1. F. Jolani, Y. Yu and Z. Chen, "Enhanced Planar Wireless Power Transfer using Strongly Coupled Magnetic Resonance," *Electronics Letters*, **51**, 2, January 22, 2015, pp. 173–175.

2. P. Si, A. P. Hu, S. Malpas and D. Budgett, "A Frequency Control Method for Regulating Wireless Power to Implantable Devices," *IEEE Transactions on Biomedical Circuits and Systems*, **2**, 1, March 2008, pp. 22-29.

3. S. Li and C. C. Mi, "Wireless Power Transfer for Electric Vehicle Applications," *IEEE Journal of Emerging and Selected Topics in Power Electronics*, **3**, 1, March 2015, pp. 4-17.

4. J. Wang , *et al*., "A Conformal Split-Ring Loop as a Self-Resonator for Wireless Power Transfer," *IEEE Access*, **8**, 2020, pp. 911-919.

5. J. Sieiro, J. M. Lopez-Villegas, J. Cabanillas, J. A. Osorio and J. Samitier, "A Physical Frequency-dependent Compact Model for RF Integrated Inductors," *IEEE Transactions on Microwave Theory and Techniques*, **50**, 1, Jan. 2002, pp. 384-392.

6. A. P. Sample, D. T. Meyer and J. R. Smith, "Analysis, Experimental Results, and Range Adaptation of Magnetically Coupled Resonators for Wireless Power Transfer," *IEEE Transactions on Industrial Electronics*, **58**, 2, Feb. 2011, pp. 544-554.

7. G. F. Liu and D. P. Taylor, "Characterization of spiral microstripline inductors," *Canadian Electrical Engineering Journal*, **10**, 3, July 1985, pp. 96-102.

8. Y. Cheng and Y. Shu, "A New Analytical Calculation of the Mutual Inductance of the Coaxial Spiral Rectangular Coils," *IEEE Transactions on Magnetics*, **50**, 4, April 2014, pp. 1-6.